

## Research Article

# Predicting Rush Skeletonweed (*Chondrilla juncea*) Dispersal by Wind within the Canyon Grasslands of Central Idaho

Sandya R. Kesoju<sup>1</sup>, Bahman Shafii<sup>2\*</sup>, Lawrence W. Lass<sup>3</sup>, William J. Price<sup>2</sup> and Timothy S. Prather<sup>3</sup>

<sup>1</sup>Irrigated Agriculture and Research Extension Center, Washington State University, Prosser, WA 99350, USA

<sup>2</sup>Statistical Programs, College of Agricultural and Life Sciences, University of Idaho, Moscow, ID 83844, USA

<sup>3</sup>Department of Plant, Soil, and Entomological Sciences, College of Agricultural and Life Sciences, University of Idaho, Moscow, ID 83844, USA

**\*Corresponding author**

Bahman Shafii, Statistical Programs, College of Agricultural and Life Sciences, University of Idaho, Moscow, ID 83844, USA, Email: bshafii@uidaho.edu

Submitted: 08 December 2014

Accepted: 21 January 2015

Published: 23 January 2015

ISSN: 2333-6668

Copyright

© 2015 Shafii et al.

OPEN ACCESS

**Keywords**

- Invasion
- Dispersal models
- Multi-layer perceptron (MLP)
- Rangeland
- Wind speed
- Wind direction

**Abstract**

Rush skeletonweed (*Chondrilla juncea* L.: Asteraceae) is a deep-rooted perennial invasive plant that infests well-drained, sandy-textured soils commonly found in the mountain foothills and canyon grasslands of the Pacific Northwest United States. The species can spread locally through rhizomes and over longer distances by wind, with its pappus-bearing seed. Our objective was to produce a dispersal model that would predict long-range movement and aid land managers in their efforts to find new populations of rush skeletonweed. A study area in the arid canyon grasslands within the Salmon River Canyon, Idaho, was used to develop a wind dispersal model for rush skeletonweed. Rush skeletonweed distribution data were from ground based surveys conducted in 1996, 1999-2001, and 2003-2012. Wind maps were created with topographic information and vegetation indices in a multi-layer perceptron (MLP) network analysis to predict average wind speed and wind direction. These maps were then incorporated into a GIS network modeling algorithm to predict seed dispersal. Algorithm settings were evaluated and optimized to match predicted dispersal maps with observed dispersal patterns. Wind dispersal maps provided information about the distance and direction of rush skeletonweed movement. In the canyon grasslands of central Idaho, rush skeletonweed seed consistently moved in the general direction of the wind. Rush skeletonweed patches were found to move within a range of 4 to 12 km in an estimated time period of 5 to 12 years, suggesting that land managers should anticipate searching for susceptible plant communities within that distance from current infestations. Dispersal within the study was predicted in the north to north-east direction at a rate of 500 to 1000 m/yr. Knowledge about dispersal distance and direction, and how they are modified by terrain, will be critical to land managers who seek to limit further expansion of invasive rush skeletonweed within Idaho and adjacent states.

**INTRODUCTION**

Rush skeletonweed (*Chondrilla juncea* L.) was likely introduced to eastern North America in contaminated grain seed brought from Europe [1]. Rush skeletonweed reduces biodiversity and forage production for both domestic and native herbivores by growing in dense monocultures and displacing native plants on rangelands [2,3]. Although it is spreading primarily on rangelands, its potential risk to agricultural crops is

also of concern as it competes aggressively with these crops for light, water, and nutrients [4,5].

Rush skeletonweed is a perennial invasive plant within Asteraceae that predominantly infests light-textured soils found in the mountain foothills and canyon grasslands of the Pacific Northwest United States. Approximately 1.2 million ha are infested in Idaho, with dispersal into adjacent Montana. Rush skeletonweed is designated as a noxious species in seven US

states (AZ, CO, ID, MT, NV, OR, and WA). The species thrives on well-drained soils and occurs at elevations from less than 225 m to over 1,830 m that receive 250 mm to 1500 mm annual precipitation [3,6].

Flowering, seed set, and dispersal of rush skeletonweed take place in the summer and continue into fall in the intermountain and Pacific Northwest regions [7,8]. Rush skeletonweed is apomictic with flowers that open in the morning, when seeds are mature and have an opportunity to disperse. Flowering occurs from mid-July until first frosts *Liao et al.*, [9]. About two weeks after flowering, seeds are fully developed and a small number of seeds have been observed to germinate three days after flowering. In July and August, seed production peaks but can continue into November. Rush skeletonweed can produce as high as 10,000 seeds per plant under field conditions [10]. Seeds are carried by wind, water, animals, machinery, and vehicles [3,11]. Most local population increase is due to vegetative regeneration, however, seed dispersal by the wind accounts for most long-range dispersal of rush skeletonweed [10].

One invasion front occurs in central Idaho, along the Salmon River canyon. Understanding dispersal along the invasion front provides land managers with knowledge critical to preventing further expansion. Although detection and delineation of weed infestations are carried out using visual observations, such methods are time- and labor intensive, particularly when trying to detect sparse infestations in remote areas. The process of detection can be made more efficient by targeting surveys based on the predicted probability of rush skeletonweed occurrence and the potential for its dispersal. Land managers can focus on sites with a high likelihood of infestation based on landscape characteristics of currently infested sites. The approach may improve both the efficiency and success of management actions such as containment and eradication.

Understanding factors that influence landscape-level vegetation patterns is critical to successful ecosystem management. An in-depth knowledge of where and at what rate a species moves across the landscape is a prerequisite to understanding seed dispersal patterns. The ability to model dispersal patterns upon the landscape would improve knowledge of rush skeletonweed movement, providing land managers with a useful management tool.

In recent years, several studies addressed the importance of seed dispersal in ecological processes [12-16]. The most important of these studies consider modeling seed dispersal using both the phenomenological approach [12,17-20] and the mechanistic approach, especially for wind dispersal [14,21-32]. Though a phenomenological approach has been favored for modeling dispersal in large-scale and long-term population studies [16,17,33], due to its inherent simplicity, it still requires plant location data for calibration, which limits the use for any new species or environmental settings [31]. Mechanistic approaches, despite their advantages of being estimated independently of the dispersal data and providing insights into the underlying transport mechanisms, still require computer-intensive simulations of wind statistics and hence are impractical for large-scale, long-term applications [31]. Seed dispersal takes place across a wide range of scales; long-distance seed

dispersal is increasingly recognized as both important and overlooked (Nathan 2006) [34]. Part of the reason long-distance seed dispersal has been neglected is that it is fundamentally a landscape-level process.

The standard empirical and mechanistic models [19,28,30,35,] which model seed movement in wind for different plant or tree species lack the ability to be applied to extensive landscapes. To address dispersal across extensive landscapes, a spatial network model algorithm has been recently used to describe dispersal in heterogeneous environments [36], and for modeling seed dispersal incorporating plant community and topography across the landscapes [37]. These algorithms anticipate long-distance dispersal considering parameters such as wind speed, wind direction, topography (slope, aspect, and elevation), and vegetation structure. It is important to develop a network representation of rush skeletonweed dispersal and find the shortest, least-cost path between two points in the network to predict rush skeletonweed dispersal and future infestations.

Rush skeletonweed is just one of the invasive plants in rangelands of the Pacific Northwest. Management of invasive species such as rush skeletonweed across extensive areas is challenging and would benefit from a landscape-level decision support tool. The purpose of this research was to produce a dispersal model that would aid land managers in their efforts to find new populations of rush skeletonweed across the landscape. The method incorporates information from a vegetation index, as well as topographical and weather variables (wind speed and wind direction) to predict rush skeletonweed dispersal.

## METHODS

### Study area

The bounding coordinates for rush skeletonweed study area were -117° to -115° longitude, and 44° to 48° latitude. Model training data was split into two regions: Region 1 (Adams, Washington, Valley, Idaho counties of central Idaho) was used for dispersal model building, while Region 2 (Latah, Benewah, Clearwater, and Nez Perce counties) was used for dispersal model validation (Figure 1). Rush skeletonweed distribution data were collected by ground-based survey crews who collected plant location data within the study area during a span of 16 years, specifically in the following years: 1996, 1999-2001, 2003, 2004-2012. The area is large so surveys conducted each year do not necessarily overlap in their coverage. Five GIS polygons, representing rush skeletonweed infestations, referred to here as areas 1 through 5, were selected from Region 1 for dispersal model building (Figure 2). The training data were selected based on the year the infestations were surveyed (older infestations were considered more desirable) as well as the polygon size (larger polygons were assumed to be older). For dispersal model validation, five additional GIS polygons from Latah and Nez Perce counties of Region 2 were selected (Figure 1). Data for dispersal model validation were selected based on the size of the infestation; polygons were more than 0.1 acres while point data were less than 0.1 acres.

### Spatial dependence model

To examine spatial patterns for rush skeletonweed

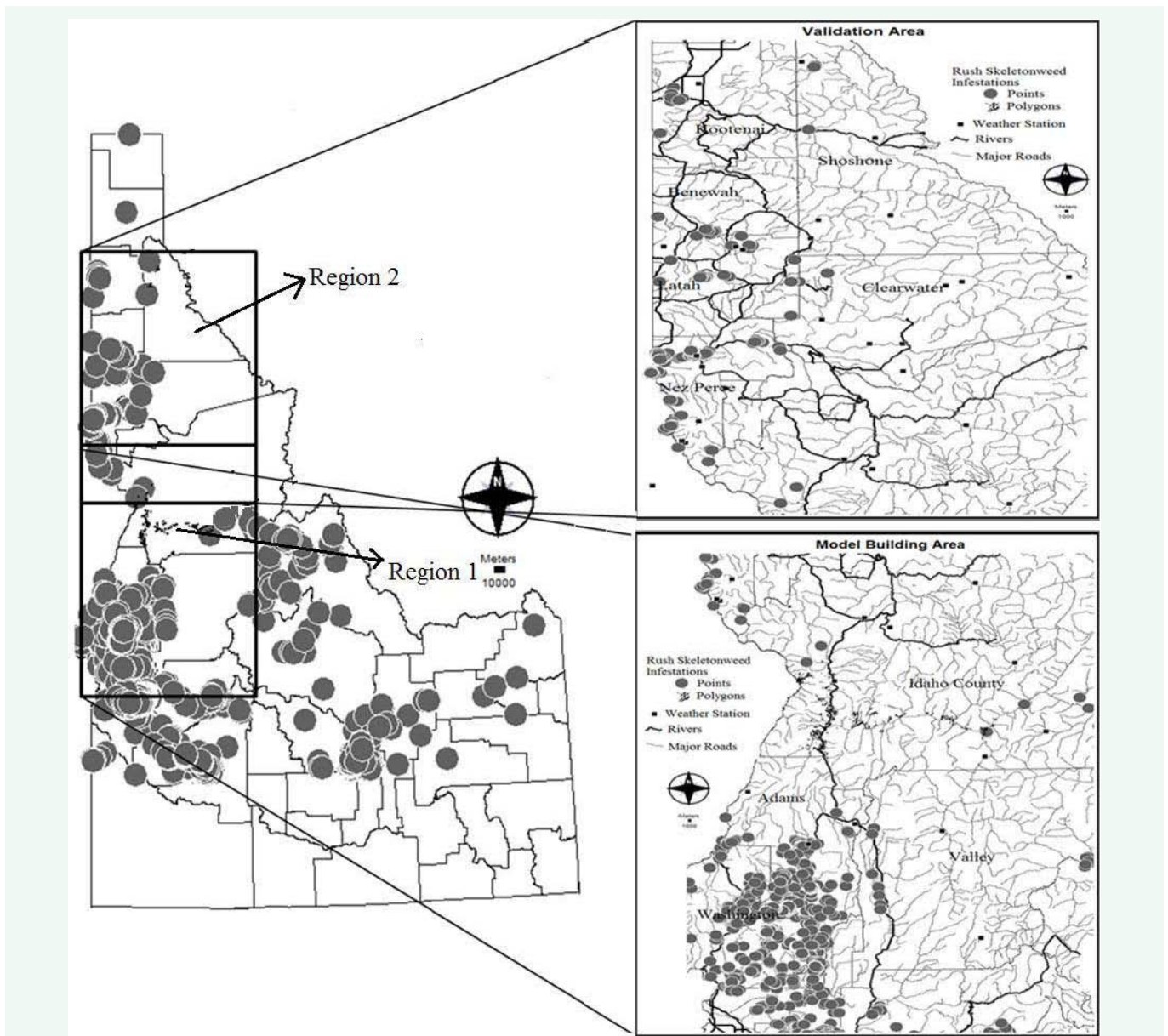


**Figure 1** Idaho map showing rush skeletonweed infestations (points in grey color, polygons and lines in black color) with two regions (Region 1 and Region 2) in black color rectangles; a) Region 1 which was used for dispersal modeling and b) Region 2 which was used for validating the dispersal model.

infestations across the Salmon River canyon and relate those to the role of wind direction in determining the potential patterns of dispersal, semivariograms were used [38,39]. According to Cressie (1993) [40] a variogram is composed of the variance between all field value pairs ( $x$  and  $y$ ) separated by a given distance,  $h$ . A complete variogram is then defined across all possible distances. The empirical semivariogram, developed from observed data, characterizes the average degree of similarity between values in different locations (rush skeletonweed infestations in this case) as a function of their separation distance as well as direction [41]. Such an empirical semivariogram can be estimated from the available data by:

$$\gamma_h = \frac{1}{2N_h} \sum (Z_{i+h} - Z_i)^2 \quad (1)$$

Where  $\gamma(h)$  is the empirical semivariance for the lag  $h$  (separation distance),  $z_i$  and  $z_{i+h}$  are the infestation values at location  $i$  and  $i+h$ , respectively, and  $N(h)$  is the number of pairs of points separated by distance  $h$ . Following computation of the empirical semivariance values, theoretical semivariance models such as the spherical, exponential [42,43], wave, power, and linear were fitted using ordinary least squares [40,41]. Each model describes spatial continuity differently based on how each increases monotonically as a function of distance. Each model can also be described by its parameters such as the range ( $a$ ), sill ( $c$ ), and nugget ( $c_n$ ) which determine the shape of the theoretical semivariogram. Variability between observations separated by very short distances is described by the nugget effect ( $\gamma$  intercept of the variogram model) [44]. The level at which a

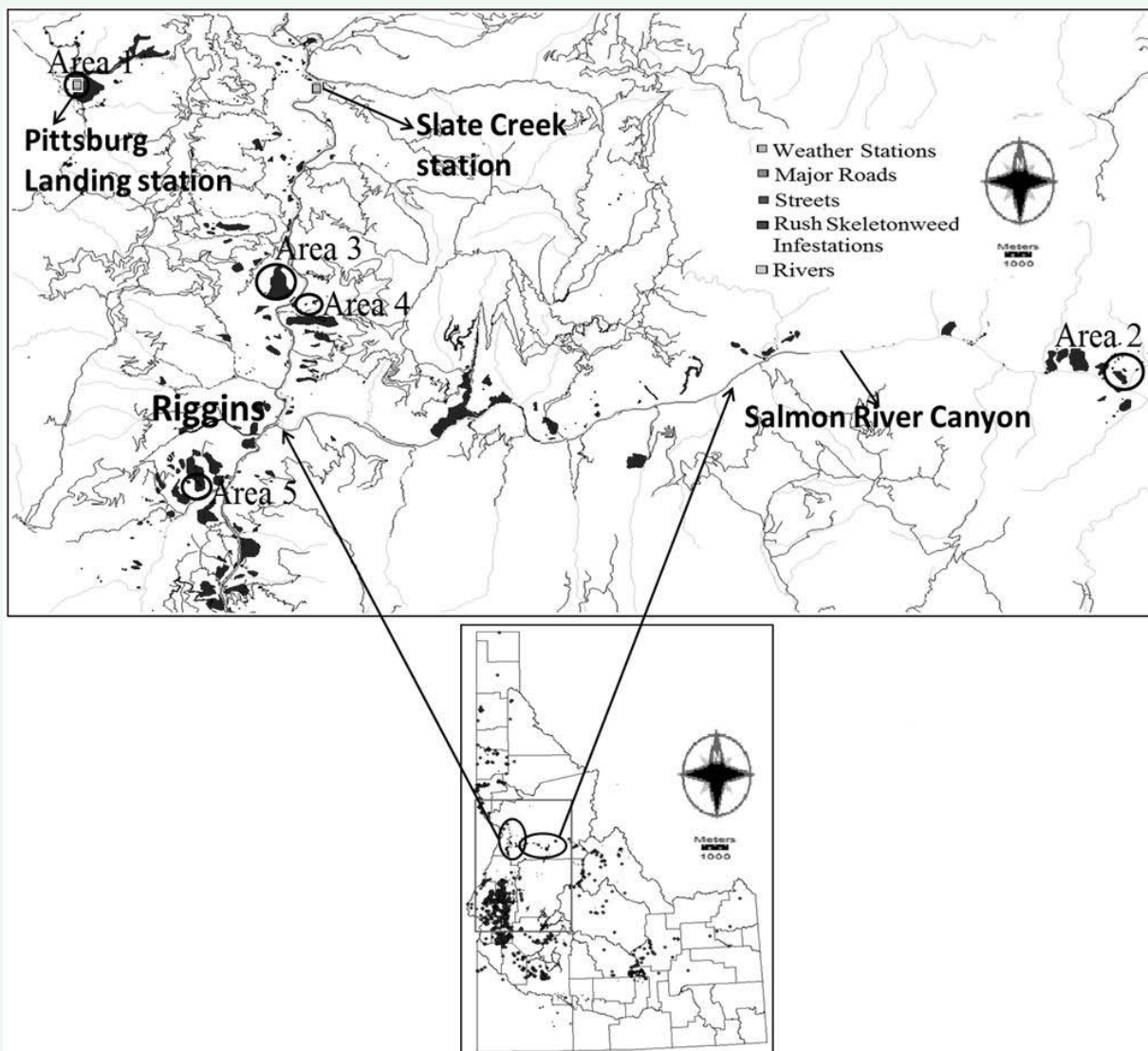


**Figure 2** Black ellipses (on inset Idaho map) indicate the study area along the Salmon River Canyon (right hand) and calibration area along the town of Riggins (Left hand), both in Idaho County, Idaho. Small circles represent five areas (1 to 5) used for dispersal model building; small light grey squares represent Pittsburg Landing and Slate Creek weather stations; black polygons or points represent rush skeletonweed infestations.

model plateaus (called the sill) represents the variance between independent and spatially uncorrelated locations. The distance at which the sill occurs is referred to as the range. The study area in and around the Salmon River was selected for use in spatial dependence modeling. In order to increase the computational efficiency, however, the area was divided into five subunits, with each being modeled separately.

### Potential characteristic variables used for rush skeletonweed wind dispersal model

Wind-dispersed mechanistic models may incorporate many factors including the effects of morphology, release heights, settling velocities, horizontal wind speeds, convection, local topography, forested trees, shrubs, and grassland forbs on diaspore movement and dispersal distance curves in (Table 1) [21,22,24,26,28,29,45,46,]. Our spatial network dispersal model considered explanatory variables such as elevation (m),

slope, aspect [37], and transformed soil adjusted vegetation index (TSAVI) [47], land surface feature shape (categorical data describing the surface of the land such as peaks, ridges, saddles, flats, ravines, pits, saddle hillsides, slope hillsides, concave- and convex hillsides or inflection hillsides), wind flow (direction flowing from a pixel), wind speed (m/s), and wind direction ( $^{\circ}$ ) (Table 1) at the spatial scale of a 10 x 10 m pixel. Remotely sensed data of the study area were acquired from LandSat 5<sup>1</sup> on July 2, 2011 and July 11, 2011 to calculate TSAVI, and landform data were calculated from Dimensional Elevation Model [48].

### Wind speed and direction data

Hourly average wind direction (degrees) and wind speed (mph) for July and August were downloaded from RAWS USA Climate Archive (<http://www.raws.dri.edu/index.html>) for weather stations which covering the study area (Idaho) as well as portions of Oregon, Washington, Wyoming, and Montana.

Anemometers in the weather stations were installed at 10 m above the ground level. The number of years used to calculate average wind speed and direction ranged from 1 to 26 depending on available records. Data from stations were removed from the analysis if average wind speed was greater than 10 m/s and the adjacent stations did not report these sustained high winds.

According to [11], between 10 and 20 days after flowering, rush skeletonweed plants begin to shed seeds which can then be carried 6 m with a wind speed of 4 m/s [49]. This study concentrated on daytime wind speed and wind direction maps for rush skeletonweed seed movement since wind direction varied considerably during nights for July, August, September, and October months (44 to 293°) when compared with the days (127° to 252°). The data files for the weather stations were merged and separated into day and night designations using the latitude-based sunrise and sunset times of each station. Data within each year were then averaged on a biweekly basis. July and August were considered the primary time period for seed production and dispersal; therefore, data from the last week of July to second week of August were used for modeling. Twenty nine weather stations were available over this time frame for

model development and twenty weather stations for model validation.

<sup>1</sup>Earth Resources Observation and Science Center, U.S. Geological Survey, Mundt Federal Building, Sioux Falls, SD. <http://lpdaac.usgs.gov>

### Wind rose plots

Wind rose plots, showing wind direction and wind speed patterns, were created to compare the consistency of the wind dispersal models with the observed wind patterns. The wind rose plots were generated for weather stations closest to the model building and model validation areas (Pittsburg Landing and Slate Creek weather stations for the model building areas, and Lapwai weather station for the validation as shown in Figure 3 and 4).

### Wind speed and direction maps

The averaged biweekly (last week of July into second week of August) data of wind speed (m/s) and wind direction (rad) were used to create the wind speed and wind direction maps using the SAS software system (SAS 1999). Bivariate polynomial interpolation with an 8-point search radius was used to interpolate values between points and make a raster

**Table 1:** Comparison of variables used in empirical/mechanistic models versus those used for the spatial network model in estimating rush skeletonweed movement.

Empirical / Mechanistic models	Spatial network model
Wind velocity (m/s), horizontal and vertical wind speed (turbulence and updrafts)	Wind speed (m/s) measured with anemometers placed at 10 m height, wind, direction
Elevation (m), release height (m)	Elevation, slope, aspect, flow, curvature at 10 x 10 m pixel size. For example if rush skeletonweed is on uphill/downhill, then release height will be taken care of by slope, elevation and curvature.
Forested trees, health land shrubs, and grassland forbs	Vegetation index considering leaf area index, vegetation height, phenology

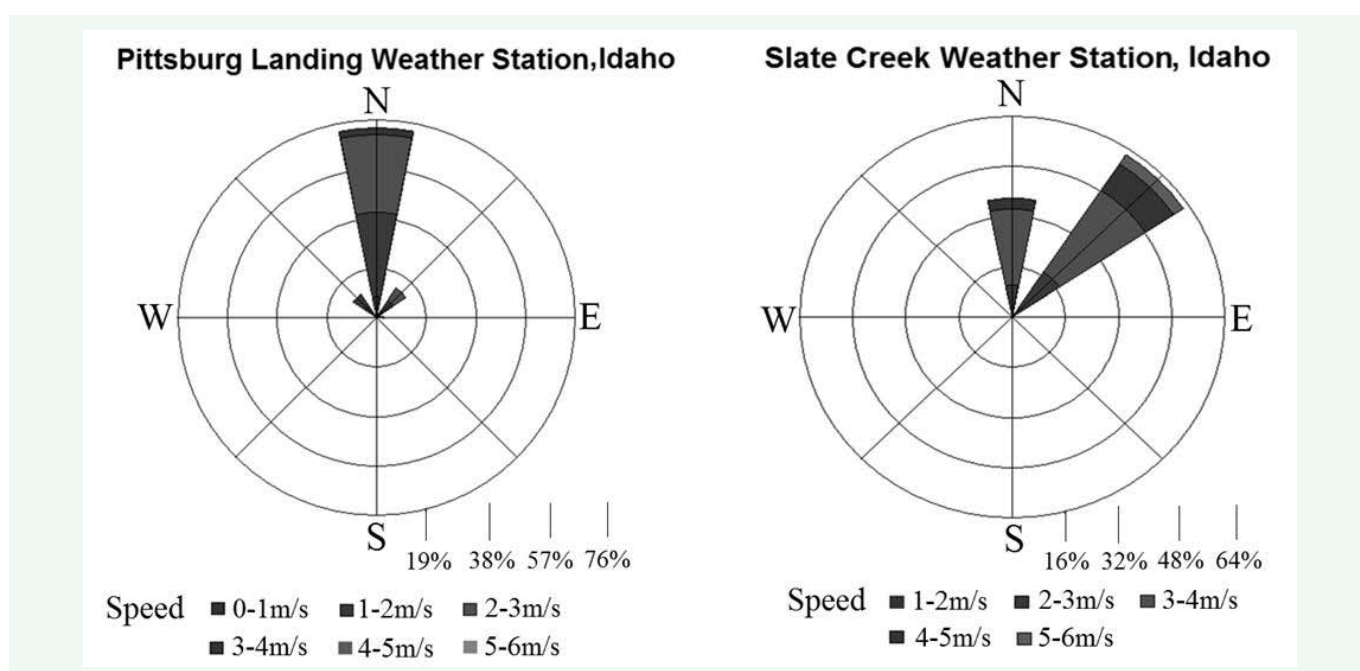


**Figure 3** Wind rose plots for wind speed and wind direction for the two weather stations located in the model building tile.

file depicting wind direction and speed with a 100 x 100 m grid. Additional grid sizes of 200 x 200 m, 300 x 300 m, and 500 x 500 m were investigated but results did not significantly differ from 100 x 100 m grids. The interpolated wind direction data were converted back to 10 x 10 m resolution and to degrees for use in the dispersal model.

Prior to defining the equations that go into a dispersal model algorithm, potential factors influence dispersal, such as wind speed, wind direction, topography (slope, aspect, and elevation etc), and vegetation structure were identified using multi-layer perceptron (MLP). The interpolated wind speed and wind direction data were adjusted for topography and vegetation using a MLP model [50]. In MLP modeling, training data are subjected to a supervised classification algorithm in order to define a spatial neural network. This process uses forward and backward propagation between the nodes (connection points) in the network until the algorithm determines the essential set of characteristics, as well as their potential interactions, necessary to describe the system [51]. For example, using a backward elimination process, starting with six explanatory variables (TSAVI, elevation, curvature, slope, flow, and aspect), several candidate models (curvature, aspect, slope, elevation, vegetation index (CASET); aspect, slope, elevation, vegetation index (ASET); slope, elevation, vegetation index (SET); and aspect, elevation, vegetation index (AET) were assessed for minimal mean squared error (MSE) as well as the structure of the underlying residuals at 10 x 10 m grid resolution. Additional grid sizes of 30 x 30 m, 50 x 50 m, and 70 x 70 m were also evaluated; however the results did not significantly differ from those of the 10 x 10 m grids.

For candidate models residuals and corresponding MSE values were calculated from predicted and observed values of each weather station. When the candidate models were compared, the AET wind speed model had the lowest MSE compared to other models (CASET, ASET, and SET respectively). Evaluation of wind direction models also showed a low MSE for

the AET model. As with wind speed, residual analysis indicated a random normally distributed residual with a mean of zero in the model building and validation regions. Hence, the AET model was selected as the final model form for predicting wind speed and direction for both the model building and validation regions.

### Dispersal modeling

The IDRISI software package module "DISPERSE" was used to model rush skeletonweed dispersal. The DISPERSE module is a spatial network analysis algorithm that utilizes images representing forces and frictions across an area of interest to model the cost of movement along a predefined grid of cells (see for example *Shafii et al. 2003*) [52]. For rush skeletonweed, the most efficient (least cost) paths from an infestation to all potential destinations was determined based on wind speed and direction inputs. The process can be evaluated at any possible position on the grid, given a cost limit or threshold total cost for movement (TTC). As part of its computations, the DISPERSE module uses a predefined cost function and an anisotropic function which determine the predicted rush skeletonweed movement through each network link. These are described below.

### Cost Function

Rush skeletonweed dispersal can be viewed as a process based on two factors: survival to seed production, and subsequent seed movement. These factors can be related to the cost of rush skeletonweed movement across a landscape (network). Generally, the cost function may be defined by:  $COST = T_s * T_m$ , where COST is the probability of existing at a given point [x,y] on the network,  $T_s$  is a component measuring the potential or probability of rush skeletonweed surviving to seed production at [x,y], and  $T_m$  is related to the probability of rush skeletonweed seed moving to point [x,y].  $T_s$  were assumed to be 100 % at this stage because we were initially interested in seed movement. The effect of variable survival rates on dispersal will be addressed in subsequent research. By assuming a complete survival, the model

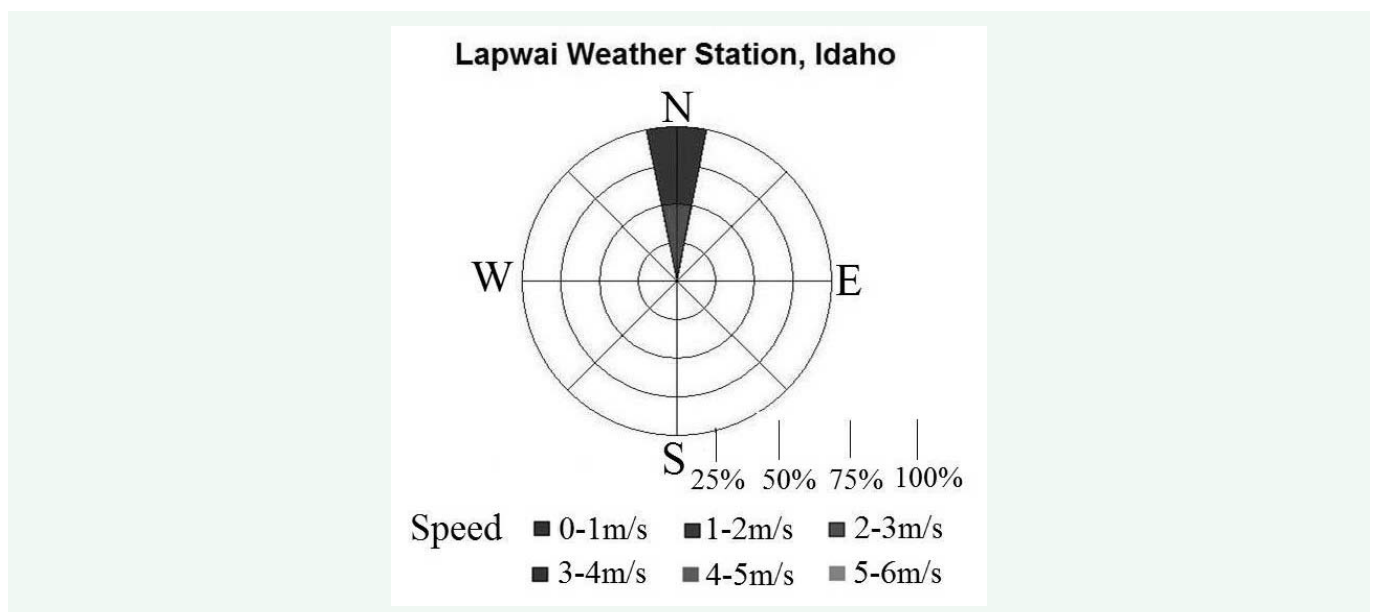
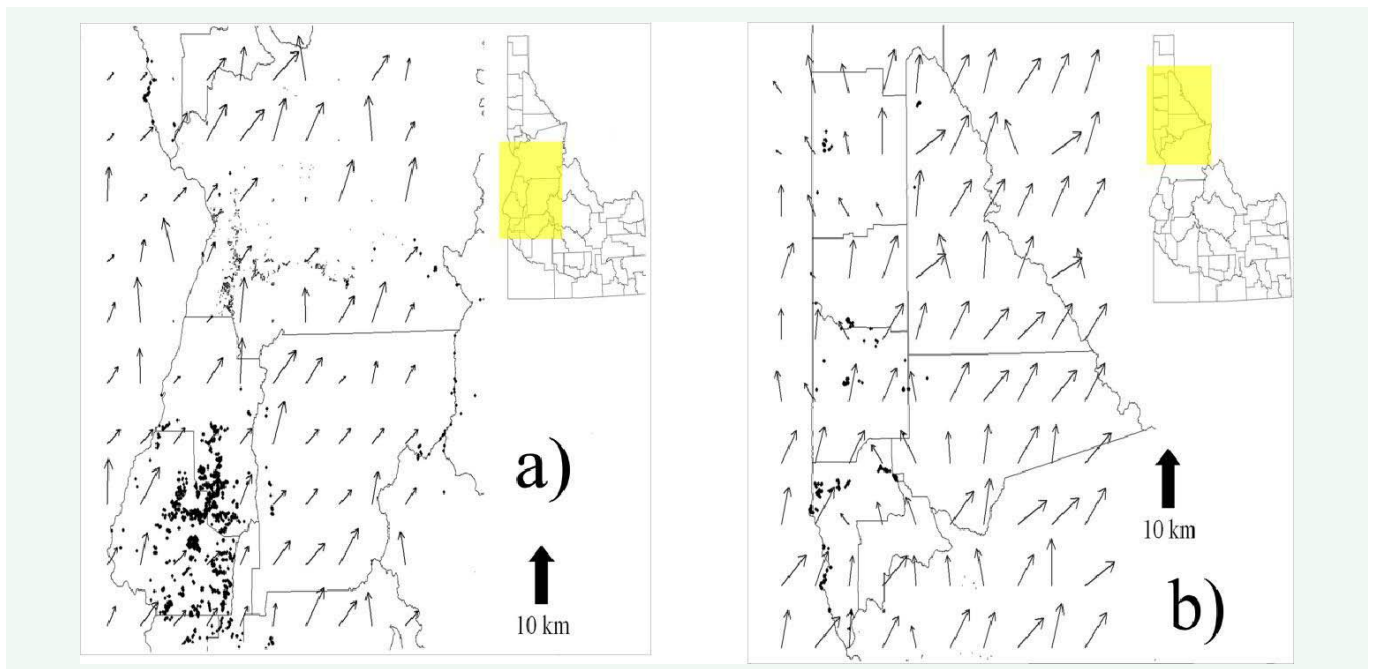
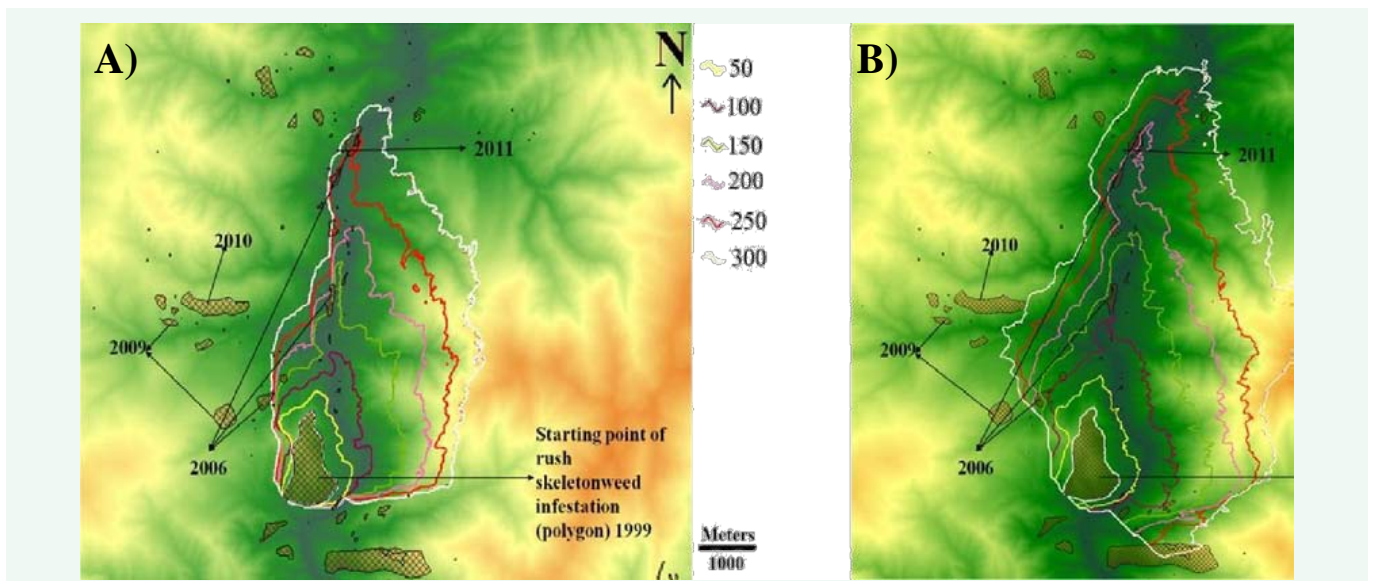


Figure 4 Wind rose plots for wind speed and wind direction for weather stations located in the validation tile.



**Figure 5** Biweekly plots indicating wind direction and magnitude (arrow and arrow length, respectively) in north central Idaho a) Region 1 b) Region 2; Rush skeletonweed infestations are in black.



**Figure 6** Dispersal model for area 3, used in the model building process. Contour lines represent 50-300 iterations of the model and are elevation map (yellow color - high elevation; dark green -low elevation). Polygons (cross hatched) represent known rush skeletonweed represents year infestations were surveyed; two angle setting scenarios are shown: a)  $k$  of 2.0; b)  $k$  of 0.5.

should produce the farthest predicted movement areas that land managers might expect in a year.

The term,  $T_M$ , is related to the probability of rush skeletonweed moving across a link in the grid representing the area of interest. For rush skeletonweed, computation of  $T_M$  utilizes both the predicted wind speed and wind direction (as forces and frictions) as described above. In theory, the network model can apply friction equally in all directions, in an isotropic manner, or the friction can change with direction, referred to as

anisotropic movement. This later method results in slower or faster movement along the grid for different directional paths. If rush skeletonweed moves along all links at the same rate then  $T_M = 1$ ; otherwise,  $T_M$  is determined as

$$T_M = 1/f, \text{ where } T_M \text{ refers to force and } f \text{ is a friction value.}$$

Here the effective friction (EF) is given as a power function, defined in IDRISI as:  $EF = (SF)^*f$ , where SF is the potential full magnitude of the friction and  $f$  is given by:

$$f = 1/\cos^k \alpha \quad (2)$$

The function in (2) above incorporates the difference between the direction of movement and the direction of the applied friction, in this case wind direction; the parameter  $k$  controls the sensitivity to the angle of the difference, which itself ranges from 0 to 90°. A value of  $k = 0$  produces the isotropic (friction is equal in all directions) model, while larger values of  $k$  lead to a higher degree of directionality within the model (anisotropic situation). All relative frictions in IDRISI software were expressed as values greater than 1 (dispersal is impeded) or as relative forces, values less than 1 (dispersal is assisted). Thus, if wind forces were considered and had a base force of 10 km/hr, a wind of 30 km/hr would be specified as a relative force of 0.33. Once cost and anisotropic functions are determined, the prediction of rush skeletonweed dispersal can be carried out through the network model algorithm.

### Creating dispersal maps

Five polygons were selected from different areas near Riggins, ID. The polygons which were dated earliest (old infestations such as infestations of 1997, 1999, and 2000) and larger in size were selected as starting points. Older and large polygon infestations were selected assuming that they were most likely responsible for satellite infestations. Vector format polygons representing the infestations in GIS were first converted to a raster graphic format where each pixel was denoted as either 0 (infestation absent) or 1 (presence of infestation). These raster images were considered as infestation sources. A predicted wind speed map from the MLP corresponding to the polygon region provided the force magnitudes while the analogous similar area of the MLP wind direction map provided the force direction information. Prior to use, the predicted wind speed map was hardened using on a logarithmic scale of the wind speed to estimate the magnitude of force (ranging from 0 to 1 expressed as relative frictions). The predicted wind direction was rotated 180° to represent a force in the model.

The results from spatial dependence model showed spatial correspondence between infestations at a distance of 250 m up-to

5000 m. Calibration of the dispersal model time steps determined that a model run of 50 time-step increments was approximately equivalent to a 1000 m dispersal distance. However, to increase the probability of detecting an infestation, this 50 iteration-step increment was extended further (one step at a time) by 100, 150, 200, 250, and 300 increments to ensure better coverage of the field surveys. Additionally, two different angle sensitivities ( $k = 0.5$  and 2.0) were used to determine the best settings for anisotropic infestation prediction.

### Dispersal model assessment

Two basic methods were used for assessing the dispersal model simulation results for model building and validation regions: 1) visual assessment and 2) omission error rates. Visual assessment is a qualitative measure of how well a predicted infestation boundary fits the corresponding observed boundary. Multiple predicted boundaries (250 or 300 iterations), each at differing costs based on magnitude and direction of force were used to assess observable trends in prediction patterns. The visual inspection, while qualitative, generally allows for quick assessment of model predictions and can be easily done by a potential user. As a more quantitative measure, the proportion of omitted infestations developed into an error matrix (omission / commission error rates) was also calculated for each of the iteration and  $k$  setting. The number of existing infestations covered by the predicted dispersal pattern at each time-step was calculated and divided by total number of existing infestations to give the proportion of coverage. The omission error rate was calculated by subtracting the proportion of coverage from 1 and represents the proportion of existing infested polygons omitted from the final predicted map.

### Dispersal model validation

Validation in this study was done to determine the adequacy of the dispersal model, and to assess whether the model is applicable to other areas in the landscape, as measured on new polygons in the validation areas. For the latter purpose, the dispersal model was applied to new infestations in Latah and Nez Perce counties (external validation) to assess future spread. The

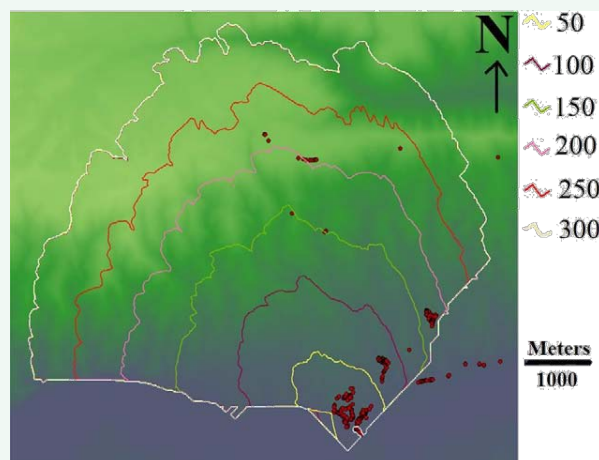


**Figure 7** Dispersal model validation for area 4 at an angle of  $k = 0.5$ . Contour lines (50-300 iterations) overlaid on digital elevation map (yellow/light green color - high elevation; dark green -low elevation) red points/polygons represent rush skeletonweed infestations.



wind dispersal model was applied to an independent area with 483 rush skeletonweed infestations on the Continental Divide between Montana and Idaho.

## RESULTS

### Spatial dependence model

The spatial arrangement of rush skeletonweed within the Salmon River Canyon offers clues into how patches of rush skeletonweed are related and if there is directionality to that relationship. Infestations of rush skeletonweed were generally oriented towards the north (N) and north-east (NE) directions i.e., at an angle of 0 - 45° along the terrain for all the five subunits (Table 2). The estimated range occurred at a lag (separation) distance of 3 km for subunit 1 suggesting that rush skeletonweed infestations were not correlated when the distance was more than 3 km. However, as the distance between infestations became smaller than this interval, there was a higher degree of correlation present. For subunit 2 and 3 rush skeletonweed infestations were correlated when the distance was less than 1 km while less than 2 km for subunit 4 and 5 km for subunit 5.

### Wind speed and direction maps

Lower wind speeds were located in forested areas in both model building and validation regions. The wind speed ranged from 0.06 m/s to 3.78 m/s for model building region and 0.60 m/s to 5.0 m/s for validation region. The predicted wind direction was moving from south (S) and south-west (SW) towards N and NE direction in model building area (Figure 5a). The predicted wind direction moves from SW across the Salmon River Canyon, and in Nez Perce forest moves from SE. In validation region the predicted wind direction moves from SE and SW (Figure 5b). The predicted wind direction was moving from SE and S towards NW and N in Latah county and while from SE and SW in Nez Perce county.

### Dispersal modeling

Wind dispersal maps provide information related to how far rush skeletonweed seeds may move and in which direction. The output from the dispersal model was converted to a predicted rush skeletonweed dispersal distance image (contour map). Contour maps for area 3 are given in Figures 6a and 6b, for example, at an angle sensitivity setting of,  $k=0.5$  and 2.0. These contours are overlaid on the corresponding elevation maps where dark blue/black colors represent lower elevations, dark to light green are intermediate elevations and yellow to orange are higher elevations. Given the change in the angle of setting ( $k = 2$  and 0.5), and equation (2), a corresponding change in the predicted boundary was observed. A visual assessment of

the dispersal model results clearly showed that an angle of  $k = 0.5$  provided a better fit than  $k = 2.0$  (Figure 6a, b). In addition, when quantitatively assessed using the omission error rate, in all five modeling areas the number of infestations omitted was fewer with a  $k$  of 0.5 compared to a  $k$  setting of 2.0 (Table 3). Nearly 90 to 100 % of known infestations were covered at 250 to 300 iterations in three of the areas tested (area 1, 2, and 5, respectively) at an angle of force,  $k = 0.5$ , while only two areas (areas 2 and 5) had equivalent coverage at a setting of 2.0. Although omission error rates were similar for both settings (Table 3), the total number of known infestations covered at  $k=0.5$  setting was higher.

In the dispersal model, rush skeletonweed seeds moved towards the N and NE directions with dispersal distances ranging from 4 to 12 km in an estimated time period of 5 to 12 years. The starting point of infestations used was 1999 when data were first recorded in the study region, and known infestations downrange from these older infestations were aged at 2006 to 2011, implying a time period of 7 to 12 years. Visual assessment suggested that at 250 to 300 iterations, the dispersal model for area 3 had broader predicted boundaries and a maximum number of known infestations covered. Similar results were seen in the other four areas (results not shown). The omission error rates were lowest at 250 - 300 iterations for all the areas (Table 3). If all five areas were considered, the maximum observed dispersal distance (from the point of infestation to the predicted boundary) was 12 km [53]. Overall, rush skeletonweed is predicted to disperse in this area at an average of 500 to 1000 m/yr towards N and NE direction. Considering the maximum number of known infestations covered and the low omission error rates over all five modeling areas, the dispersal model was found to be good in predicting rush skeletonweed seed movement. The predicted dispersal in these areas was consistent with the wind rose plots directions, where the nearest weather stations (Pittsburg Landing and Slate Creek) showed a maximum wind speed in the N and NE direction (Figure 3).

### Dispersal model validation

Estimated rush skeletonweed dispersal in the validation areas were in N and NW directions with dispersal distances ranging from 3.4 to 6.5 km. Due to the lack of adequate temporal data of rush skeletonweed infestations in validation area, only the spatial validation was considered. Visual assessments suggested that at 250 iterations, the dispersal model for area 4 had broader predicted boundaries and covered the maximum number of known infestations (Figure 7). Results were similar for the other four validation areas [53]. Additionally, the omission error rates were 1 to 10 % for 100-300 iterations compared to a 50 iteration setting where error rates ranged from 10 to 90

**Table 2:** Model parameters obtained from the semivariogram procedures.

	Model	Sill	Range	Nugget	Direction (degrees)
Subunit 1	Spherical	0.2887	4899.7	NA	45
Subunit 2	Gaussian	0.0757	432.4	NA	0
Subunit 3	Exponential	0.0392	264.4	NA	0
Subunit 4	Wave	0.0231	271.7	0.0127	45
Subunit 5	Wave	0.0449	352	0.0210	0

% (Table 4). If all five areas were considered, the maximum observed dispersal distance was 6.5 km from point of infestation to the predicted extent of 250-300 iterations. In the validation analyses, 100-300 iterations were more adequate in predicting rush skeletonweed seed movement for all the five areas based on the maximum number of known infestations covered and low proportion of omission rates. Seed movement for all the areas was in the NW direction except area 4 which was towards N direction and which was also found to be inconsistent with the nearest weather station, Lapwai, where the wind speed was in the N and NE directions (Figure 4).

Finally, the dispersal model at the 250 to 300 time-step range resulted in 80-90 % coverage of known infestations and captured the pattern of seed movement for the five areas. The distance of seed dispersal ranged from 4 to 12 km and consistently moved in the general direction of the wind for the canyon grasslands of central Idaho. Overall, dispersal model results for model building and validation areas showed similar results in relation to the maximum number of known infestations coverage and proportion of omission error rates, with the exception of the dispersal pattern and directionality in relation to wind rose plots for a few areas. The wind rose plots for weather stations in the validation area were not always within the same location as the validation sites, and weather station data time series was shorter for some validation weather stations than in the model development weather stations. The main reasons for observing deviated directionality patterns in the validation area might be insufficient spatial and temporal data in a polygon format, and limited weather station data.

### Application of wind dispersal model to an independent study area

The wind dispersal model was applied to an independent area with 483 rush skeletonweed infestations on the Continental Divide between Montana and Idaho. Rush skeletonweed locations

were mapped using GPS by members of the weed management unit. Results showed that the wind dispersal model links 90 % of the infestations when projected seed dispersal was 2 km (omission error 10.56 %, Table 5). The model further indicated that nearly all infestations (99.6 %) could be linked by wind at predicted dispersal distance of 12 and 14 km. These results were used by ground crews to identify new infestations on the Continental Divide. The model was also applied to two additional independent sites in the Idaho Frank Church Wilderness and Idaho Clearwater National Forest, achieving the same level of accuracy.

### DISCUSSION

Spatial dependence distance ranged from 250 m to 5000 m and demonstrated an anisotropic pattern from 0 to 45° over all of the five subunits. The anisotropic pattern was found consistent with wind rose plots for Pittsburg Landing and Slate Creek weather stations with wind moving towards N and NE corresponding with rush skeletonweed dispersal. The sill and the range parameters for each of the structures varied suggesting that the spatial correlation was not consistent for the five subunits. The most likely reason for the difference in ranges was that rush skeletonweed seeds moved in the direction of wind due to topographical factors [28,54]. The differing speeds that occurred in the N and NE direction may have been responsible for the variance. The nugget effect was greater than zero in subunits 4 and 5, meaning that observations separated by extremely small distances were dissimilar [44]. This dissimilarity may have resulted from seed dispersal, germination, mortality events that occurred at scales smaller than 2-5 km, local changes in topography, or could simply be the result of sampling error. The slope of the semivariogram in relation to direction was not consistent in the five subunits, suggesting that the pattern of the infestations changed with the subunits. The results indicated a strong effect of canyon orientations and are likely due to local wind patterns within the canyon grasslands. Results also

**Table 3:** Omission error rates (%) at two different angle settings ( $k = 2.0, 0.5$ ) for the five model building areas.

Areas with Starting point of infestation (year)	Iterations at $k = 2.0$						Iterations at $k = 0.5$					
	50	100	150	200	250	300	50	100	150	200	250	300
Area 1 (1999)	87.5	62.5	37.5	12.5	12.5	0.00	90.9	63.6	54.5	18.2	9.10	0.00
Area 2 (2001)	89.5	84.2	42.1	26.3	5.30	0.00	90.9	68.2	31.8	9.10	0.00	0.00
Area 3 (1999)	97.1	77.1	54.3	28.6	11.4	0.00	96.4	73.2	57.1	41.1	21.4	0.00
Area 4 (1997)	88.9	66.7	61.1	38.9	27.8	0.00	89.5	78.9	71.1	60.5	28.9	0.00
Area 5 (2000)	85.7	78.6	64.3	14.3	0.00	0.00	85.0	70.0	35.0	15.0	10.0	0.00

**Table 4:** Omission error rates (%) of known infestation for the model building and validation areas.

Starting point of infestation (year)	Iterations for Model Building Area						Iterations for Validation Area					
	50	100	150	200	250	300	50	100	150	200	250	300
Area 1	92.0	92.0	46.0	31.0	8.00	0.00	90.0	13.0	0.00	0.00	0.00	0.00
Area 2	89.0	79.0	53.0	16.0	0.00	0.00	13.0	0.00	0.00	0.00	0.00	0.00
Area 3	94.0	74.0	57.0	32.0	21.0	0.00	21.0	19.0	17.0	1.00	1.00	0.00
Area 4	75.0	69.0	63.0	63.0	25.0	0.00	34.0	7.00	7.00	4.00	0.00	0.00
Area 5	95.0	80.0	50.0	40.0	30.0	0.00	83.0	83.0	83.0	50.0	50.0	0.00

**Table 5:** Omissional error rate (%) and number of rush skeletonweed infestations at various distances.

Distance (km)	Infestations linked	Omissional error (%)
0	0	100.00
1	386	20.08
2	432	10.56
4	452	6.42
6	470	2.69
8	474	1.86
10	476	1.45
12	481	
14	481	0.41

Total number of infestations = 483

provided justification for inclusion of wind as a variable for dispersal model.

Wind dispersal models offer a management tool for forecasting the direction of movement. Though rush skeletonweed can spread vegetatively and through seeds dispersed by animals, vehicles, machinery, and water, [3] reported that wind currents were more important than other factors in influencing long distance dispersal. [49] conducted wind tunnel experiment on rush skeletonweed and found that pappus bearing seeds can disperse 6 m with a wind speed of 4 m/s [11] reported rush skeletonweed can disperse 24 to 32 km/yr.

The rush skeletonweed dispersal models predicted a long distance dispersal from 4 to 12 km within a time period of 5 to 12 years. Modeling studies of seed flight have shown that turbulence increase dispersal distances because structured turbulent eddy motions tend to lift seeds to higher elevations with higher horizontal wind speeds [30]. According to [28], diaspores reaching steep hillsides gain altitude relative to ground surface greatly increase the flight times and considerably increase dispersal distances. Wind speeds and updrafts in open habitats and forests are important in moving the seeds long distances [29,35]. When seeds are dispersed in dense vegetation, such as Nez Perce forest, the wind speed decreased, thereby reducing the dispersal distance [55], while [28] reported that a pappus bearing diaspore can disperse > 100 m when the terminal velocity is <1.5 m/s in open habitats. Our landscape-level approach resulted in predictions of yearly dispersal distance consistent with [28,29]. Horizontal wind speed increases with height above ground and the nature of this effect depends on surface roughness, as recognized in most small-scale meteorological dispersal models.

Models are needed that relate dispersal distances to such measurable parameters as wind speed and direction, which thereby allow comparisons among different environments. Long-distance dispersal may be due mainly to the topographic effects [28], and if the topographic effects are not considered, they may considerably underestimate dispersal of infestations by wind [19,23]. Models incorporating wind directionality describe seed dispersal data better than other theoretical models, such as exponential or Weibull functions, which did not have this ability [56]. Taking these conclusions into account, the dispersal model provides additional evidence that incorporating elevation,

aspect, vegetation index, and wind parameters into dispersal enables better prediction of long-distance dispersal of seeds or pollen on large-scale and long-term population dynamics. The landscape approach moves dispersal modeling to an application level to inform land managers where an invasive, wind-dispersed species may move.

We addressed how seeds could disperse but we did not address survival once seeds are moved to new sites. According to [57], rush skeletonweed's prolific nature of seed production and the ability of the seed to disperse over considerable distances results in wide-spread dispersal even with a very small percentage of seedling success. [4] found that dispersed rush skeletonweed seeds have no innate dormancy and 95 % of rush skeletonweed seeds germinated. Without dormancy and with high germinability, the site conditions where rush skeletonweed seed exists determine establishment after seed movement. Rush skeletonweed seedling establishment is highly variable from site to site and year to year [58], depending on soil moisture and burial depth. Prediction of rush skeletonweed occurrence will therefore require use of landscape characteristics. A complete picture of rush skeletonweed will need to incorporate an occurrence model (survival) into the dispersal process in order to refine model predictions and subsequently help land managers understand how far and in which direction rush skeletonweed can be expected to move. Until those components are developed, however, the current dispersal model provides useful predictions of rush skeletonweed movement and helps narrow the focus of control efforts.

In summary, knowledge of where and at what rate an invasive species such as rush skeletonweed moves across a landscape is often limited or nonexistent. Using a spatial network model algorithm, we produced a wind dispersal model that would aid land managers in their efforts to find new populations of rush skeletonweed across the canyon grasslands of central Idaho. Rush skeletonweed patches were related up to distances of 4 to 12 km, suggesting that land managers should survey distances of at least 12 km from the current infestations towards the N or NE. The region considered for this study displayed a large degree of topographic relief. There are steep canyons interspersed with flatter areas, as well as forested areas with grassy expanses. Local conditions that modify wind patterns likely result in a range of distances where rush skeletonweed patches are related. By using topographic features in addition to wind patterns, predicted bounds for rush skeletonweed movement allows managers to meet their objectives for limiting further rush skeletonweed expansion within Idaho and other adjacent states. The wind maps developed here may also benefit management efforts. A 4 to 12 km distance suggests there are local conditions that result in this range of distances.

## ACKNOWLEDGMENTS

This research was supported in part by the USDA CSREES Integrated-National Research Initiative Competitive Grants Program. Number 2008-02991.

## REFERENCES

1. Piper GL, Coombs EM. Fire conditions pre- and post-occurrence

- of annual grasses on the Snake River Plain. Stephen BC, Peters EF. Proceedings Ecology and Management of Annual Rangelands. Boise. 31-36
2. Carroll P. Wiry skeletonweed threatens Oregon agriculture, Rangelands. Rangelands archives. 1980; 2: 21.
  3. Sheley RL, Hudak JM, Grubb RT. Rush Skeletonweed. Sheley RL, Hudak JM. Rush Skeletonweed: A Threat to Montana's Agriculture. Montana State Univ. Publ. EB-132, Bozeman, MT. 1995; 318-323
  4. Schirman R, Robocker WC. Rush skeletonweed-threat to dryland agriculture. Weeds. 1967; 15: 310-312.
  5. Zimdahl RL. Weed crop competition. Int. Plant Protection Center, Corvallis, Ore.1980.
  6. Moore RM. Chondrilla juncea L. (Skeletonweed) in Australia. Proceedings 7th British Weed Control Conference. 1965; 2: 563-568.
  7. Hitchcock CL, Cronquist A. Flora of the Pacific Northwest. Seattle, WA: University of Washington Press. 1973; 730.
  8. Bussan AJ, Dyer WE. Herbicides and rangeland. In: Sheley, Roger L, Petroff JK, eds. Biology and Management of Noxious Rangeland Weeds. Corvallis: Oregon State University Press. 1999; 116-132 p.
  9. Liao JD, Martin SB, Val Jo A, Shaw L. Seed biology of rush skeletonweed in sagebrush steppe. Journal of Range Management. 2000; 53: 544-549.
  10. Jacobs J, Goodwin K, Ogle D. Plant Guide for rush skeletonweed . USDA-Natural Resources Conservation Service, Montana State Office, Bozeman. 2009.
  11. McVean DN. Ecology of Chondrilla juncea L. in south-eastern Australia. Journal of Ecology. 1996; 54: 345-365.
  12. Clark JS, Silman M, Kern R, Macklin E, HilleRisLambers J. Seed dispersal near and far: patterns across temperate and tropical forests. Ecology. 1999; 80: 1475-1494.
  13. Nathan R, Muller-Landau HC. Spatial patterns of seed dispersal, their determinants and consequences for recruitment. Trends Ecol Evol. 2000; 15: 278-285.
  14. Nathan R, Horn HS, Chave J, Levin S. Mechanistic models for tree seed dispersal by wind in dense forests and open landscapes. Seed dispersal and frugivory: ecology, evolution and conservation. CABI, Wallingford. 2001.
  15. Cain ML, Nathan R, Levin SA. Long-distance dispersal. Ecology. 2003; 84: 1943-1944.
  16. Levin SA, Muller-Landau HC, Nathan R, Chave J. The ecology and evolution of seed dispersal: a theoretical perspective. Annual Review of Ecology Evolution and Systematics. 2003; 34: 575-604.
  17. Clark JS. Why trees migrate so fast: confronting theory with dispersal biology and the paleorecord. Am Nat. 1998; 152: 204-224.
  18. Clark J, Horvath L, Lewis M. On the Estimation of Spread Rate for a Biological Population. Statistics and Probability Letters. 2001; 51: 225-234.
  19. Bullock JM, Clarke RT. Long distance seed dispersal by wind: measuring and modeling the tail of the curve. Oecologia. 2000; 124: 506-521.
  20. Higgins SI, Nathan R, Cain ML. Are long-distance dispersal events in plants usually caused by nonstandard means of dispersal? Ecology. 2003; 84: 1945-1956.
  21. Okubo A, Levin SA. A theoretical framework for data analysis of wind dispersal of seeds and pollen. Ecology. 1989; 70: 329-338.
  22. Greene DF, Johnson EA. A model for wind dispersal of winged or plumed seeds. Ecology. 1989; 70: 339-347.
  23. Greene DF, Johnson EA. Long-distance wind dispersal of tree seeds. Canadian Journal of Botany. 1995; 73:1036-1045.
  24. Greene DF, Johnson EA. Wind dispersal of seeds from a forest into a clearing. Ecology. 1996; 77: 595-609.
  25. Horn HS, Nathan R, Kaplan SR. Long-distance dispersal of tree seeds by wind. Ecological Research. 2001; 16: 877-885.
  26. Nathan R, Safriel UN, Noy-Meir I. Field validation and sensitivity analysis of a mechanistic model for tree seed dispersal by wind. Ecology. 2001; 82: 374-388.
  27. Nathan R, Katul GG, Horn HS, Thomas SM, Oren R, Avissar R, et al. Mechanisms of long-distance dispersal of seeds by wind. Nature. 2002; 418: 409-413.
  28. Tackenberg O. Modeling long-distance dispersal of plant diaspores by wind. Ecological Monographs. 2003; 73: 173-189.
  29. Tackenberg O, Poschlod P, Kahmen S. Dandelion seed dispersal: the horizontal wind speed does not matter for long-distance dispersal - it is updraft. Plant Biology. 2003; 5: 451-454.
  30. Soons MB, Heil GW, Nathan R, Katul GG. Determinants of long-distance dispersal by wind in grasslands. Ecology. 2004; 85:3056-3068.
  31. Katul GG, Porporato A, Nathan R, Siqueira M, Soons MB, Poggi D, et al. Mechanistic analytical models for long-distance seed dispersal by wind. Am Nat. 2005; 166: 368-381.
  32. Pazos GE, Greene DF, Katul G, Bertiller MB, Soons MB. Seed dispersal by wind: towards a conceptual framework of seed abscission and its contribution to long-distance dispersal. Journal of Ecology. 2013; 101: 889-904.
  33. Chave J, Levin S. Scale and scaling in ecological and economic systems. Environmental and Resource Economics. 2003; 26: 527-557.
  34. Nathan R. Long-distance dispersal of plants. Science. 2006; 313: 786-788.
  35. Nathan R, Katul GG, Bohrer G, Kuparinen A, Soons MB, Thompson SE, et al. Mechanistic models of seed dispersal by wind. Theoretical Ecology. 2011; 4: 113-132.
  36. Fortuna MA, Gómez-Rodríguez C, Bascompte J. Spatial network structure and amphibian persistence in stochastic environments. Proc Biol Sci. 2006; 273: 1429-1434.
  37. Lass LW, Prather TS, Shafii B, Price WJ. Tracking invasive weed species in rangeland using probability functions to identify site-specific boundaries: A case study using yellow starthistle (*Centaurea solstitialis* L.). In GIS Applications in Agriculture. CRC Press. 2011; 277-299.
  38. Donald WW. Geostatistics for mapping weeds, with a Canada thistle (*Cirsium arvense*) patch as a case study. Weed Science. 1994; 42: 648-657.
  39. Heisel T, Andreasen C, Ersboll AK. Annual weed distributions can be mapped with kriging. Weed Research. 1996; 36: 325-336.
  40. Cressie NAC. Statistics for Spatial Data. New York: John Wiley & Sons. 1993.
  41. Rossi RE, Mulla DJ, Journel AG, Franz EH. Geostatistical tools for modeling and interpreting ecological spatial dependence. Ecological Monographs. 1992; 62: 277-314.
  42. Webster R, Oliver MA. Statistical Methods in Soil and Land Resource Survey. Oxford University Press, New York, USA. 1990.
  43. Deutsch CV, Journel AG. GSLIB: Geostatistical Software Library and User's Guide, Oxford University Press, New York. 1992.

44. Isaaks EH, Srivastava RM. An introduction to applied geostatistics. Oxford University Press, New York, 1989;516.
45. Verkaar HJ, Schenkeveld AJ, van de Klashorst MP. The ecology of short-lived forbs in chalk grasslands: Dispersal of seeds. *New Phytology*. 1983; 95: 335-344.
46. Andersen M. Mechanistic models for the seed shadows of wind-dispersed seeds. *American Naturalist*. 1991; 137: 476-497.
47. Baret F, Guyot G, Major DJ. TSAVI: A vegetation index which minimizes soil brightness effects on LAI and APAR estimation. *Geoscience and Remote Sensing Symposium, IGARSS'89. 12th Canadian Symposium on Remote Sensing*. 1989; 3:1355-1358.
48. Gesch DB. The National Elevation Dataset. In: *Digital Elevation Model Technologies and Applications: The DEM Users Manual*. Maune D editor. 2nd Edition: Bethesda, Maryland, American Society for Photogrammetry and Remote Sensing. 2007; 99-118.
49. Hensen I, Muller C. Experimental and structural investigations of anemochorous dispersal. *Plant Ecology*. 1997; 133: 169-180.
50. Sreelakshmi K, Ramakanth KP. Neural networks for short term wind speed prediction. *World Academy of Science, Engineering and Technology*. 2008; 42: 721-725.
51. Atkinson PM, Tatnall ARL. Neural networks in remote sensing. *International Journal of Remote Sensing*. 1998; 18: 699-709.
52. Shafii B, Price WJ, Prather TS, Lass LW, Thill DC. Predicting the likelihood of yellow starthistle (*Centaurea solstitialis*) occurrence using landscape characteristics. *Weed Science*. 2003; 51: 748-751.
53. Kesoju SR. Modeling wind dispersal of rush skeletonweed (*Chondrilla juncea* L.) in the canyon grasslands of central Idaho. University of Idaho. 2012.
54. Rossi RE, Mulla DJ, Journel AG, Franz EH. Geostatistical tools for modeling and interpreting ecological spatial dependence. *Ecological Monographs*. 1992; 62: 277-314.
55. Thiede DA, Augspurger CK. Intraspecific variation in seed dispersion of *Lepidium campestre* (Brassicaceae). *American Journal of Botany*. 1996; 83: 856-866.
56. Tufto J, Engen S, Hindar K. Stochastic Dispersal Processes in Plant Populations *Theor Popul Biol*. 1997; 52: 16-26.
57. Kinter C L, Meador BA, Shaw NL, Hild AL. Postfire invasion potential of rush skeletonweed (*Chondrilla juncea*). *Rangeland Ecology and Management*. 2007; 60: 386-394.
58. Cullen JM, Groves RH. The population biology of *Chondrilla juncea* in Australia. *Proceedings of the Ecological Society Australia*. 1977; 10: 121-134.

#### Cite this article

Kesoju SR, Shafii B, Lass LW, Price WJ, Prather TS (2015) Predicting Rush Skeletonweed (*Chondrilla juncea*) Dispersal by Wind within the Canyon Grasslands of Central Idaho. *Int J Plant Biol Res* 3(1): 1026.